A practical method to account for random phase approximation effects on the dynamic scattering of multi-component polymer systems

M. Monkenbusch (iD), M. Kruteva (iD), M. Zamponi, L. Willner (iD), I. Hoffman, B. Farago, and D. Richter

View Online **Export Citation** **CrossMark**

ARTICLES YOU MAY BE INTERESTED IN

A practical method to account for random phase approximation effects on the dynamic scattering of multi-component polymer systems

View Online Export Citation CrossMark

M. Monkenbusch,[1,a] (iD) M. Kruteva,[1] (iD) M. Zamponi,[2] L. Willner,[1] (iD) I. Hoffman,[3] B. Farago,[3] and D. Richter[1]

AFFILIATIONS

[1] Forschungszentrum Jülich GmbH, Jülich Centre for Neutron Science (JCNS-1) and Institute for Complex Systems (ICS-1),
52425 Jülich, Germany
[2] Forschungszentrum Jülich GmbH, Jülich Centre for Neutron Science at MLZ, Lichtenbergstr. 1, 85748 Garching, Germany
[3] Institut Laue-Langevin (ILL), 71 Avenue des Martyrs, 38000 Grenoble, France

[a] Author to whom correspondence should be addressed: m.monkenbusch@fz-juelich.de

ABSTRACT

Investigations of polymer systems that rely on the interpretation of dynamical scattering results as, e.g., the structure factor $S(Q, t)$ of single chains or chain sections may require the inclusion of effects, as described within the framework of the random phase approximation (RPA) for polymers. To do this in practice for the dynamic part of $S(Q, t)$ beyond the initial slope is a challenge. Here, we present a method (and software) that allows a straightforward assessment of dynamical RPA effects and inclusion of these in the process/procedures of model fitting. Examples of applications to the interpretation of neutron spin-echo data multi-component polymer melts are shown.

Published under license by AIP Publishing. https://doi.org/10.1063/1.5139712

I. INTRODUCTION

Dynamics of polymer chains, parts of polymer chains, or other objects such as stars, dendrimers, and various block copolymers, embedded in different polymeric environments, is a vital information to understand the physical behavior and material properties of those systems.[1] As for structural information, the accessibility of a detailed dynamics insight depends on the possibility to create contrast between the selected constituents of the system. For most polymers, this can be performed by selectively deuterating some components in combination with thermal neutrons as a scattering probe. The thus generated coherent scattering intensity is usually observed in small angle neutron scattering (SANS) experiments and conveys structural information on chain correlations and conformations. Analyzing this scattering intensity with the help of neutron spin-echo (NSE) spectroscopy yields further information on the temporal development of the corresponding structural features. Thus mobilities, lifetimes of certain structures, or aggregates can be inferred, and further analysis yields information on interactions, forces, friction/dissipation, and topological restrictions.[2] In the early days, the

focus of such an investigation lies on the single chain dynamics of homopolymers.[3,4] The visibility generating contrast was between chemically identical (up to the H vs D replacement) chains, usually 10%–20% protonated chains in a "matrix" of deuterated chains. In these cases, the dynamical scattering functions are not altered by the interference of chains, which can be described by the random phase approximation (RPA).[5–7] The sole RPA-type effect is the form of the concentration (volume fraction ϕ) dependence of the common intensity factor $\phi(1 - \phi)$.

As soon as one moves a step toward more heterogeneous systems, genuine RPA-type influences on the scattering functions beyond trivial factors can become important. Even a simple binary mixture can be affected. This may immediately be realized by assuming a hypothetical scenario in which the above mentioned h/d polymer mixture, e.g., the d-polymer, is of a different kind and virtually immobile such that it forms a stiff network hosting the mobile h-chains. If in the SANS regime all are described in terms of scattering densities, the coherent scattering of such a system stays completely elastic. Despite the fact that the h-chains may be quite mobile (or may even constitute a kind of solvent), no relaxation or decay of

the wavevector Q and time t dependent intermediate scattering function $S(Q, t)$ will be observed. Of course, the transition to the conventional homogeneous system upon gradually turning on the mobility of the immobile part will lead to a gradual approach of the constant $S(Q, t)$ toward the conventional relaxing single chain structure factor. Intermediate situations will yield some intermediate relaxation behavior. The aim of the here presented formalism is to devise a tool to get a quantitative access to this property. The main effect as described by the RPA approach here is typically not the minor influence of more or less small interaction parameters χ but the drastic exclusion interaction which is built in by the volume conservation condition.

Before going into detail, it should also be emphasized that the following treatment basically serves to take into account these types of correlations that influence the visibility of dynamical structure functions. It will not contribute anything to the changes and peculiarities of genuine changes in the dynamics of the constituents of the system due to interactions with their surroundings. However, the singling out of the "decoration" effects of the chain arrangement of the dynamic signal enables an undistorted view on the proper chain dynamics.

II. RPA THEORY

As early as 1967, Jannink and de Gennes applied a dynamic RPA approach to semidilute polymer solutions,[5] where the theoretical basis of the algorithms was outlined. The procedure elaborated in this paper is based on the treatment described by Eqs. (8)–(18b) in the work of Akcasu et al.,[6,7] where explicit expressions for the relation between the Laplace transforms of the undisturbed/free/genuine scattering functions of the different constituents of the system and the scattering function of the interacting and labeled sample are given. The practical difficulty in applying this scheme, which was formulated already 25 years ago, is not the arithmetic between the Laplace transforms but the translation from the model functions into that space and the efficient and accurate backtransform to the (Q, t) space of experimental data.

A. Non-interacting multi-component RPA

Here, we explicitly discuss and implement the RPA expressions for a system of $n + 1$ (interacting) components, a matrix (polymer), and n (different) polymers with different contrasts with respect to the matrix/solvent. This leads to a $n \times n$ matrix problem. In the static formulation, this implies that

$$\mathbf{S}(Q)^{-1} = \mathbf{S^0}(Q)^{-1} + \mathbf{v}(Q), \tag{1}$$

where $\mathbf{S^0}(Q)$ is the matrix of undisturbed scattering functions and $\mathbf{v}(Q)$ describes the interaction between the components. With that, the scattering intensity $I(Q)$ obtained for a specific contrast $\mathbf{a}$ is

$$I(Q) = \mathbf{a^T S}(Q)\mathbf{a}. \tag{2}$$

To yield the Laplace transform of the dynamic scattering matrix $\mathbf{S}(Q, s)$, Akcasu and Tombakoglu[7] defined a frequency and Q-dependent diffusion coefficient by

$$\mathbf{S}(Q, s) = \left[\mathbf{1}s + Q^2\mathbf{D}(Q, s)\right]^{-1}\mathbf{S}(Q), \tag{3}$$

i.e.,

$$\mathbf{D^0}(Q, s) = \frac{1}{Q^2}\left(\left[\mathbf{S^0}(Q, s)\mathbf{S^0}(Q)^{-1}\right]^{-1} - \mathbf{1}\right), \tag{4}$$

and derived the relation between the undisturbed/free diffusion coefficient $\mathbf{D^0}(Q, s)$ and the RPA influenced $\mathbf{D}(Q, s)$ as follows:

$$\mathbf{D}(Q, s) \simeq \left[\mathbf{1} + Q^2\mathbf{D^0}(Q, s)\mathbf{S^0}(Q)\mathbf{v'}(Q, s)\right]^{-1}$$
$$\times \mathbf{D^0}(Q, s)\left[\mathbf{1} + \mathbf{S^0}(Q)\mathbf{v}(Q)\right], \tag{5}$$

with

$$\mathbf{v'} = (\beta/s)\left[\chi_{cc}^0(Q, s)^{-1} - \chi_{cc}^0(Q, s = 0)^{-1}\right]\mathbf{EE^T} \tag{6}$$

($\beta = 1/k_B T$ will cancel out from the final expression), where $\mathbf{EE^T}$ is a matrix with all elements equal to 1 and the index cc relates to the "invisible" embedding, e.g., the deuterated matrix compound/solvent in a polymer mixture. The dynamic susceptibility $\chi(Q, s)$ relates to the scattering functions via $\chi(Q, t) = -\beta dS(Q, t)/dt$, i.e., $\chi(Q, s) = -\beta[sS(Q, s) - S(Q, t = 0^+)]$. With $\mathbf{v}(Q) = (\beta/\chi_{cc}^0)\mathbf{EE^T} + \boldsymbol{\varepsilon}$, these equations suffice to compute the dynamic RPA result over the full time range from the undisturbed dynamic structure functions $S_{ii}^0(Q, t)$ of the components to the matrix function $S_{cc}^0(Q, t)$. For the inclusion of the important interference effects resulting from incompressibility, the small interaction parameters $\varepsilon_{i,j}$ may be ignored; in particular, this applies virtually to any system composed of h- and d-labeled chains, possibly with different lengths, topology, or partial labeling schemes of the same polymer.

In this paper, we treat the general structure of the resulting matrix elements for a 3 component system (2 possibly labeled polymers +1 matrix polymer): with the short notation,

$$\mathscr{S}_i = \phi_i S_{ii}^0(Q), \tag{7}$$

and the Laplace transforms,

$$S_{ii}^0(Q, s) = S_{ii}^0(Q) F_i(Q, s), \tag{8}$$

as expressed by the Q-dependent, normalized function $f_i = F_i(Q, s)$. For the here presented procedure, it is general to express $f(s)$ in the form

$$f(s) = \left(\sum_{i=1}^N A_i\right)^{-1} \sum_{i=1}^N \frac{A_i}{r_i + s} \tag{9}$$

by which any relaxation (or even damped oscillation) type model function can be represented to virtually any desired accuracy [see Sec. III and Eq. (15) ff]. Furthermore, we have for the volume fractions $\phi_1 + \phi_2 + \phi_3 = 1$ (c = 3).

With the expression for a common denominator $\mathscr{N}$, the matrix elements of the Laplace transformed scattering matrix $\mathbf{S}$ are obtained. We have

$$\mathscr{N} = (\mathscr{S}_1 + \mathscr{S}_2 + \mathscr{S}_c)\left[\mathscr{S}_2 (f_2 s - 1) + (f_1 s - 1)\mathscr{S}_1 + \mathscr{S}_c (f_c s - 1)\right], \tag{10}$$

and with that, the matrix elements

$$S_{11} = \frac{\mathscr{S}_1}{\mathscr{N}} \times \left[f_1 (f_2 s - 1) \mathscr{S}_2^2 + f_2 (f_1 s - 1) \mathscr{S}_2 \mathscr{S}_1 + f_c (f_1 s - 1) \mathscr{S}_c \mathscr{S}_1 \right.$$
$$\left. + f_1 (f_2 s + f_c s - 2) \mathscr{S}_c \mathscr{S}_2 + \mathscr{S}_c^2 (f_c s - 1) f_1 \right] \quad (11)$$

and

$$S_{22} = \frac{\mathscr{S}_2}{\mathscr{N}} \times \left[f_2 (f_1 s - 1) \mathscr{S}_1^2 + f_2 (f_1 s + f_c s - 2) \mathscr{S}_1 \mathscr{S}_c \right.$$
$$\left. + f_1 (f_2 s - 1) \mathscr{S}_1 \mathscr{S}_2 + f_c (f_2 s - 1) \mathscr{S}_2 \mathscr{S}_c + \mathscr{S}_c^2 (f_c s - 1) f_2 \right]. \quad (12)$$

In addition,

$$S_{12} = S_{21} = \frac{-\mathscr{S}_1 \mathscr{S}_2}{\mathscr{N}} \left[(f_1 f_2 s - f_1 - f_2 + f_c) \mathscr{S}_c \right.$$
$$\left. + f_2 \mathscr{S}_1 (f_1 s - 1) + f_1 \mathscr{S}_2 (f_2 s - 1) \right]. \quad (13)$$

III. NUMERICAL IMPLEMENTATION

The Laplace transform of the resulting structure factor matrix consists of algebraic expressions that contain the Laplace transforms of the free scattering functions $\mathscr{S}_{nm}^0(Q,s)$ [Eqs. (10)–(13)]. These algebraic expressions can easily be computed once the Laplace transforms of the undisturbed function have been created. However, the difficulty consists in performing the inverse Laplace transform as the final step to arrive at the resulting intermediate structure functions $S_{nm}(Q, t)$. The present approach takes advantage from the fact that the time dependence of virtually all intermediate scattering functions that occur in the realm of soft matter and neutron spin-echo investigations can accurately be described by a rather limited number N of simple exponentials. In practice, $N = 4$–6 usually is more than enough. This applies to both free model functions and data from NSE experiments. Thus, using

$$\mathscr{L}\{\exp(-at)\} = \int_0^\infty \exp(-at) \exp(-st)dt = \frac{1}{a+s}, \quad (14)$$

the Laplace transform of the model functions can simply be written in the form of Eq. (9) as

$$\mathscr{S}_{nm}^0(Q,s) \simeq \mathscr{L}\left\{ \sum_{i=1}^N A_i \exp(-r_i t) \right\} = \sum_{i=1}^N \frac{A_i}{r_i + s}, \quad (15)$$

which even embraces the improbable cases with damped oscillation contributions by allowing complex rate parameters r_i ($\mathscr{R}(r_i) > 0$).

Having the algebraic expressions for $\mathscr{S}_{nm}^0(Q,s)$, it is straightforward to insert the free functions from Eq. (15), which after some more or less tedious algebra evidently leads to resulting structure factor matrix elements that can be represented by quotients of two polynomials, i.e.,

$$L(s) = \frac{\sum_{i=0}^{N-1} z_i s^i}{\sum_{i=0}^N c_i s^i} = \frac{Z(s)}{N(s)}. \quad (16)$$

In that case, the inverse Laplace transform of $F(s)$ is

$$\mathscr{L}(t) = \sum_{j=1}^N \frac{\sum_{i=0}^{N-1} z_i \alpha_j^i}{\sum_{i=0}^N i c_i \alpha_j^{i-1}} e^{\alpha_j t}, \quad (17)$$

where α_j is the j-th (complex) zero (with respect to s) of the denominator in Eq. (16). While the above may appear as an attractive

analytic path to the inverse, it turns out that if the degree of the involved polynomials is larger than 3, the numerics (determining zeroes and evaluating values) is problematic. In fact, for $N \leq 3(4)$, analytic expressions can be obtained; however, for generality, we use the following numerical approach.

Fortunately, the form in which the Laplace transform is available, a stable and accurate inversion by numerical integration, is possible. The analytic form allows the evaluation of the expression for $L(s) = \mathscr{S}_{nm}^0(Q,s)$ for complex s opening the route to a general, fast, and accurate inversion of the Laplace transform by

$$S_{nm}(Q, t) = \int_{\eta-i\infty}^{\eta+i\infty} \exp(st) \mathscr{S}_{nm}^0(Q,s)ds, \quad (18)$$

with η as a parameter that can be chosen to any value larger than the largest value of $-\mathscr{R}(r_i)$. Since the always decaying relaxation functions considered here have an upper bound of $-\mathscr{R}(r_i) < 0$, any value $\eta \geq 0$ may be chosen.

For the numeric inversion, the routines computing $L(s)$ from s must do this with full complex arithmetic. The integration is performed on a path $s = i\omega + \eta$ from $\omega = -\infty$ to $+\infty$. Of course, the limits have to be finite, but sufficiently large. η can be set to virtually zero.

While integration with the general adaptive integration yields robust results, it requires a huge number of iterations and therefore is slow. Another approach to the integration takes into account the general relaxation type feature of the result functions and extends the ideas of Filon.[8] It proceeds as follows:

- Setup a logarithmically spaced interval set $\{\omega_l = \omega_1, \ldots, \omega_N\}$. The first interval starts at $\omega_1 = +\varepsilon$ (virtual zero) to the first genuinely non-zero point ω_2, and the last interval ends at $\omega_N = 2\omega_{N-1}$, i.e., 2 times its starting value. In the current implementation, we use 900 intervals from $\omega = 10^{-7}$ to 10^6 (time unit = 1 ns) as default to cover all practical cases. The shift property of the Laplace transform ($F(s+a) = \mathscr{L}\exp(-as)f(t)$) implies that keeping a minimum rate $r_i > r_{min}$ for all components of the model function to avoid the singularity at $s = 0$ just adds a negligible extra decay to the curves, which is less than $r_{min}\tau_{max}$ in the experimental range from 0 to τ_{max}.
- Determine an interpolation of the form

$$S_{nm}(Q, s = i\omega + \eta) = s_{nm}(\omega) \simeq \sum_{j=-3}^2 c_j^l \omega^j \quad (19)$$
$$\text{for} \quad \omega_l < \omega < \omega_{l+1}$$

using $j_{max} - j_{min} + 1$ equally spaced support points in the interval under consideration.
- The cosine integral is then obtained by the c_j weighted sum of the analytically known cosine-integrals $B_j(t) = \int f_j(\omega) \cos(\omega t)d\omega$ of the test functions $f_j(\omega) = \omega^j$.
- With the once created list of c_j^l for all intervals, the integral sum for any t is orders of magnitude faster than the direct integration approach. Both methods yield consistent values,
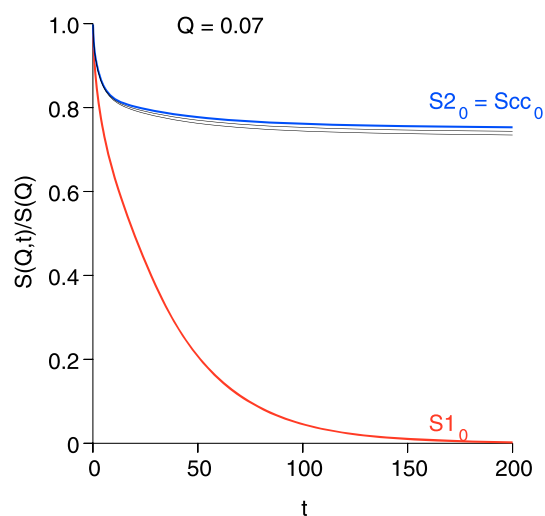
$$S_{nm}(Q, t) \simeq \sum_{l=1}^{N-1} \sum_{j=-3}^2 c_j^l [B_j(t, \omega_{l+1}) - B_j(t, \omega_l)]. \quad (20)$$
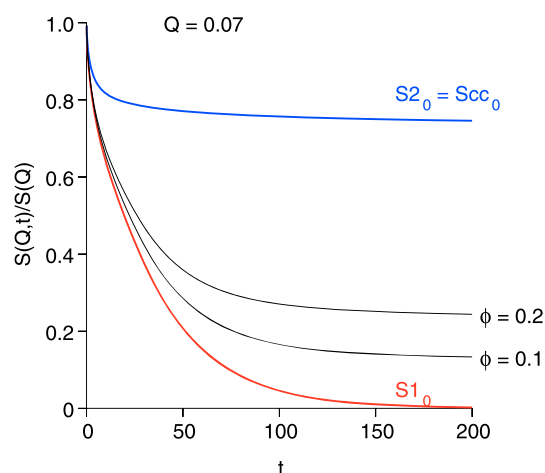
FIG. 1. Example showing the RPA effect on the scattering signal of a small diffusing Rouse chain in a matrix of long chains in the reptation regime. The red curve shows the undisturbed scattering function of the small chains $S1_0$, the blue curve shows that of the long chains $S2_0 = Scc_0$, and the black curves are the observable signals from labeled small chains at various concentrations ϕ in this system.

- Depending on the nature of the problem (i.e., in particular, if very long relaxations play a role), it is important to start the intervals at sufficiently small values; the default choice should be adequate for most NSE-related cases.

Figures 1 and 2 show examples for the outcome of the RPA-procedure for a mixture of short diffusing Rouse chains in an

FIG. 2. Example showing the RPA effect on the scattering signal of a long chain in a matrix of long chains in the reptation regime diluted by short Rouse chains. The red curve shows the undisturbed scattering function of the small chains $S1_0$, the blue curve shows that of the long chains $S2_0 = Scc_0$, and the black curves are the observable signal from 20% labeled long chains in this system with 10% and 20% (non-labeled) short chains. In this case, the influence of the RPA effect is also visible, but comparatively small, and the black curves are only slightly below the pure long chain function.

entangled long chain matrix for different concentrations of the short chains [using Eqs. (21), (22), and (A4), respectively, for the undistorted S_0 functions]. Figure 1 shows the situation where the short chains are labeled, whereas Fig. 2 pertains to 20% labeled long chains. It is clearly visible that in particular the observable short chain scattering is significantly influenced by slow long chain contributions even for concentrations of $\phi = 0.1$ and less. The influence in the case of labeled long chains is less pronounced but—if not accounted for—would also lead to errors in the inferred "plateaus" in the relaxation function of the long chain component. Note that the here shown results only account for the effect of interference due to incompressibility, and any influence of the small chain dilution on the genuine chain dynamics must be contained in the S_0 functions. Using the RPA scheme, however, allows for undistorted viewing and fitting of these functions. In a recent experiment, the salient features of these RPA predictions could be corroborated, as is reported in Sec. IV.

IV. EXPERIMENTAL VERIFICATION

To test the predictions of the RPA model treatment, we conducted an experiment at the refurbished spin-echo spectrometer IN15 at the ILL, Grenoble, on short polyethylene (PE) chains in a melt of long PE-chains at different concentrations.[9] The sample consisted of h-PE chains with about 200 monomers (M_n = 2.9 kg/mol) and a deuterated matrix polymer (d-PE) with about 2700 monomers per chain (M_n = 45 kg/mol). The volume fractions ϕ of the short chains were 0.02, 0.06, 0.12, and 0.24. Data were collected for 3 scattering angle settings corresponding to momentum transfers Q = 0.05, 0.08, 0.12 Å^{-1} and covering a time range between t = 0.05 and 477 ns using neutron wavelengths of 10 and 13.5 Å. The temperature was T = 509 K as in all previous NSE experiments on PE.[10–12] Background scattering as measured from a sample of pure long d-PE chains has been subtracted.

The long chains are well entangled, and their scattering functions are well established.[11] An interpolating representation of them is used as a pure undisturbed matrix function entering the RPA treatment (see Appendix A). While the plain de Gennes expression used in Ref. 11 can describe the PE system reasonably well over the complete NSE time range, it fails to do so for other polymers [e.g., polyisoprene (PI) or polyethyleneoxide (PEO)]. In all entangled linear polymer systems for which NSE experiments are available even at the shortest measured times ($\simeq$ 0.1 ns), the scattering function deviates from a simple Rouse behavior. However, all experimental data can accurately be described by an interpolation expression, the general form of which is motivated by the de Gennes treatment.[13] While a rigorous derivation of the expression and a straight physical interpretation of the parameters are still missing, it is possible (for all our currently available data of entangled polymers) to perfectly describe the experiments over the whole time range ($\simeq$0.1 to $\simeq$200–600 ns) and the typical momentum transfer range Q = 0.05–0.15 Å^{-1} simultaneously with only 3–4 fit-parameters. Thus, safe and accurate interpolations of $S(Q, t)$ to any (Q, t) value within the covered range, and to a certain extent, extrapolation beyond that, are enabled using this description. For the present investigation, we choose this description to represent the pure scattering function of the long chains. The necessary parameters are extracted from previous NSE experiments on long chain PE.[11,12]

The behavior of the short chains in the entangled long chain matrix is the original subject of the investigation and thus *a priori* is unknown. Mainly a modified center-of-mass diffusion, hindered by the matrix, is expected, and at larger Q, the internal dynamics of the short chains may contribute.

Naively, we may assume that the internal dynamics of the short chains is not altered by the embedding in the long chain matrix, and the pure scattering function of the short chains could be described by internal Rouse dynamics using explicit summation of finite chain modes,[14]

$$f_{\text{Rouse}}^{\text{int}}(Q,t) = \sum_{m,n} e^{-\frac{1}{6}|n-m|Q^2 l^2} \, e^{-\frac{4R_g^2 Q^2}{\pi^2} \Sigma_p \frac{1}{p^2} \cos\left(\frac{p\pi n}{N}\right) \cos\left(\frac{p\pi m}{N}\right)\left(1-e^{-p^2 t/\tau_R}\right)}. \tag{21}$$

This yields an estimate of the amount of internal dynamics to be expected; at lower Q, its influence is small.

Thus, we have $S(Q,t) = e^{-\frac{Q^2}{6}\langle r_{\text{com}}^2(t)\rangle} f_{\text{Rouse}}^{\text{int}}(Q,t)$ with—as suggested by the shape of the experimental results—a modified center-of-mass diffusion with an initial sublinear regime ($\langle r_{\text{com}}^2(t)\rangle \propto t^\beta$, $\beta < 1$) with a transition to normal (Fickian) diffusion ($\langle r_{\text{com}}^2(t)\rangle = 6D_0 t$) around a mean squared displacement (MSD) of $\langle r_{\text{com}}^2(t_0)\rangle = r_0^2$,

$$r_{\text{com}}^2(t) = \left[\left(e^{-\ln\left(\frac{r_0^2}{6D_0}\right)\beta} r_0^2 \, t^\beta\right)^a + (6\,D_0\,t)^a\right]^{\frac{1}{a}}, \tag{22}$$

where a determines the abruptness of the transition (here, we use $a = 8$).

Up to $Q \leq 0.08$ Å^{-1}, the estimated internal mode contributions stay below 25%. Therefore, we restrict the experimental assessment of the RPA effect influence to the $Q = 0.05$ and 0.08 Å^{-1} settings, where we have reliable descriptions for both the matrix and the short chain pure $S(Q,t)$ functions.

It is expected that the center-of-mass diffusion of the short chains is hindered by the long chains and therefore deviates from the Rouse expectation. In addition, simulations and experiments on similar systems yield a region of sublinear diffusion between the (here neglected) ballistic regime at very short times and Fickian diffusion at long times.[15–19] Here, we use the lowest concentration data to determine the diffusion parameters: D_0, β, and r_0^2. The thus observed short chain dynamics (pure) at low Q is dominated by the sublinear/linear diffusion.

In Figs. 3 and 4, the comparison of model calculations based on the RPA-procedure for concentrations between $\phi = 0.02$ and 0.24 is shown. The lowest concentration served to determine the parameters of the sublinear diffusion. At higher concentrations (notably at 24%), the pure function of the long chains must be modified and the diffusion of the short chains accelerates (from about 1.6 Å^2/ns to 2.6 Å^2/ns). The modification of the long chain function pertains to an increase in the tube diameter and a modification of the local reptation regime.[20] However, the differences between the NSE spectra for $\phi = 0.02$–0.12 are dominated by the RPA-related effects, and admixtures of the slow dynamics of the matrix chains become increasingly obvious with increasing concentration. Even at $\phi = 0.02$, there are small deviations from the pure undisturbed scattering function, as shown by the dashed limiting curves for $\phi \to 0$ in Fig. 4.
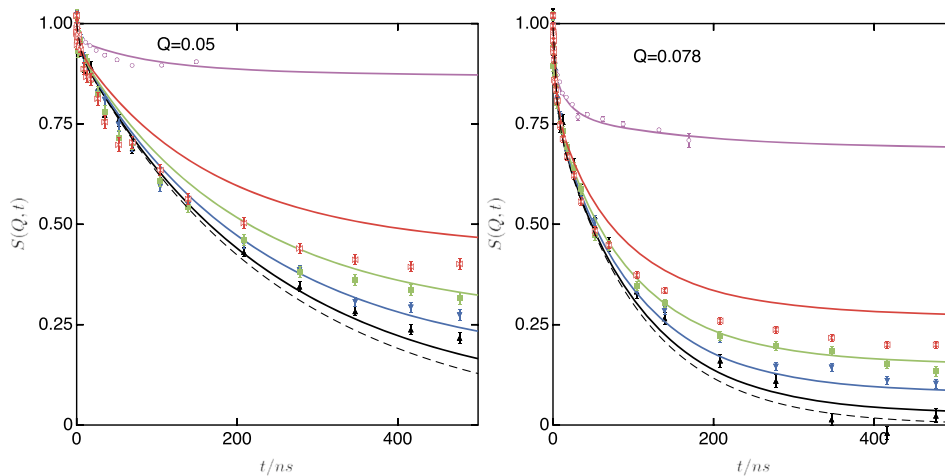
The short chain scattering function at larger Q (i.e., 0.12 Å^{-1}) deviates from the simple description in Eqs. (21) and (22). Since the detailed investigation of the genuine polymer dynamics is beyond the scope of this paper, we restrict the discussion of the RPA effect on the observed NSE scattering curves and their relation to the genuine polymer scattering functions to the data for $Q = 0.05$ and 0.08 Å^{-1}.

A full analysis of the dynamics of this polymer system will be given elsewhere as soon as the data with contrast on the long chains are also available.

The best way to grasp the scattering function of both components in a mixed system at any significant concentration levels would be to simultaneously fit experimental data both from labeled short chains in a deuterated matrix and labeled matrix chains in a melt
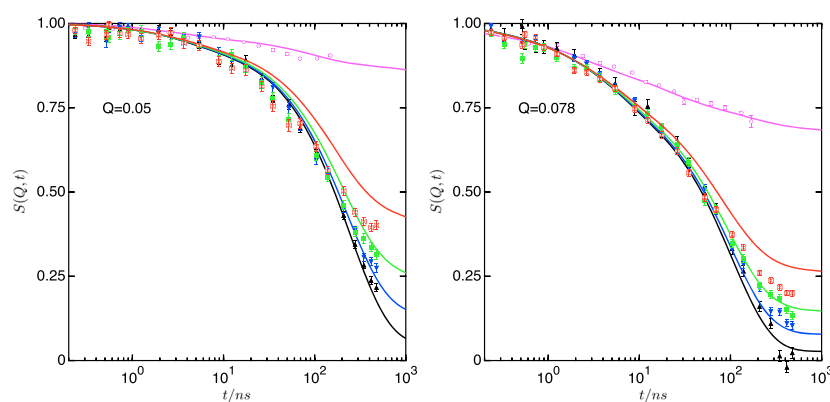
FIG. 3. NSE data from short labeled PE chains in a long 45 kg/mol deuterated PE melt. Curves comprise a combined model fit to the 2% (black), 6% (blue), and 12% (green) data in order to estimate the undisturbed short chain scattering function. The lines show the computed $S(Q,t)$ using one set of pure functions for short and long chains including the RPA effects. The parameters used to model the short chains $S(Q,t)$ by Eqs. (21) and (22) were $Wl^4 = 7 \times 10^4$ Å^4/ns, $R_e = 34.9$ Å, $D_0 = 1.68$ Å^2/ns, $r_0^2 = 698$ Å^2, and $\beta = 0.66$ for the computation of all shown curves. Note the increase in long time levels. The 24% short chain data (red) already show an obvious dilution effect and therefore deviate from the model prediction. The purple circles represent older data on long chain linear PE (see Appendix A), and the lines show the used pure long chain scattering functions as used in the RPA formalism.

FIG. 4. The same data as in Fig. 3, but on linear t-scale. In addition, the dashed line indicates the pure short chain scattering function as expected for virtual zero concentration.

of deuterated short and matrix chains with the same composition of chains with a different architecture. In addition, thus, changes in the "matrix" chain scattering function could also be accurately accessed.

V. CONCLUSION

Applying the RPA (basically the incompressibility condition) to a polymer mixture shows that for mixtures of constituents with heterogenic dynamic response the scattering signal from a labeled compound may significantly differ from its genuine (pure) scattering function. In this paper, we describe a procedure and a software implementation of it to quantitatively assess this effect and extract or fit the pure scattering functions from experimental results at finite concentrations. A proof of principle experiment on short labeled polyethylene (PE) chains in a melt of long entangled PE chains corroborates the predictions of the RPA procedure. The effects in the scattering signal stem from implicit decoration of the matrix chains by the scattering contrast of the labels. Any changes in the intrinsic dynamics either of the long or of the short chains are not described by the RPA-procedure but must be accounted for in the model function of the pure compounds. In fact, the RPA procedure allows an unbiased fitting of either or both of these pure scattering functions. However, to be sensitive to the details of both functions (at least), two experiments with labels either on the "target" or on the matrix molecules are highly desirable. In that case, both functions can be extracted without bias by using the procedure presented in this paper.

A. Implementation

The described numerical procedures have been implemented as the Fortran code. This also contains the routines to compute the here used models for the undistorted scattering functions [Eqs. (21) and (22) (short chains) and (A4) (long chains)]. Other models for undistorted scattering functions can easily be added. An interface is supplied that allows us to incorporate the method in Python programs. The code can be accessed at https://jugit.fz-juelich.de/neutron/RPA_for_polymers.

APPENDIX A: PARAMETRIZATION OF SCATTERING FUNCTIONS FOR ENTANGLED POLYMERS

In Ref. 13, de Gennes considered the density correlation along a 1-dimensional stretched "tube," which corresponds to a diffusion equation along the tube. It results in the Green function of simple diffusion, the fluctuation amplitude is $\propto \sqrt{B}$, and the average density is $\propto \sqrt{A}$,

$$\Sigma(s,t) = A + \frac{B}{\sqrt{4\pi t}} \exp\left(-\frac{s^2}{4t}\right). \quad (A1)$$

Equation (A1) is written in terms of scaled time t and length s variables in order to keep the expressions simple. In the physical application, the scale factors are input parameters.

Then, the structure factor of a Gaussian coiled tube is

$$S_{lr} = \frac{1}{L} \int_0^L \int_0^L \Sigma(s_1 - s_2, t) \exp\left[-\frac{q^2}{6}|s_1 - s_2|\right] ds_1 ds_2, \quad (A2)$$

$$S_{lr}(q,t) = \frac{1}{L\sqrt{\pi}q^4}\left(72\,A\sqrt{\pi}\left\{\exp\left[-\frac{Lq^2}{6}\right] + \left[\frac{Lq^2}{6} - 1\right]\right\} \right.$$
$$+ B\left\{2\sqrt{t}q^4\left[\exp\left(-\frac{2Lq^2 + 3L^2}{12t}\right) - 1\right]\right.$$
$$+ \sqrt{\pi}\left(\frac{q^2 t}{3} + L\right)q^4 \exp\left(t\frac{q^4}{36}\right)\left[\text{erfc}\left(\frac{q^2\sqrt{t}}{6}\right)\right.$$
$$\left.\left.\left. - \text{erfc}\left(\frac{q^2\sqrt{t}}{6} + \frac{L}{\sqrt{4t}}\right)\right]\right\}\right). \quad (A3)$$

Note that the q wave vector is with respect to the length scale a and $L = Z$ is the number of entanglements, i.e., $q \to Q\,a$ and $t \to t/\tau$, where τ sets the time scale.

The normalized scattering function $F_{lr} = S_{lr}(q, t)/S_{lr}(q, 0)$ depends on the ratio B/A only (thus, setting $A = 1$, we are left with the parameter $B \to B/A$). In de Gennes' treatment, $B = 1/3$, which is also used in our parametrized description of the long chain scattering functions. The essence of this parametrized description is then the diffusive density fluctuation Eq. (A1) along the tube (local

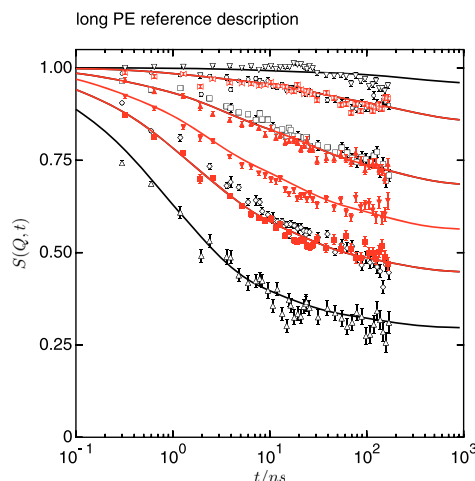reptation), however, with adapted length a and time τ scaling parameters.

The full scattering function is then constructed as a product of the expression for a finite Rouse chain ($M_w \simeq M_e$) by direct summation with an effective rate $W_x l^4$ as a parameter and without c.o.m. diffusion multiplied by Eq. (A3) with the length and time scales a and τ as parameters,

$$S(Q,t)/S(Q) = S_{lr}(Qa, t/\tau)/S_{lr}(Qa, t=0)$$
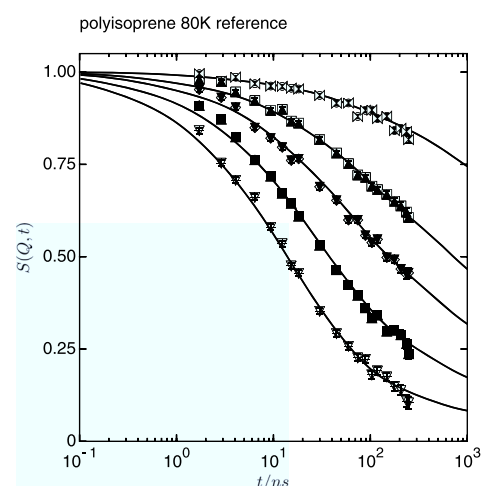$$\times S_{Nrouse}^{N=N_e}(Q,t)/S_{Nrouse}^{N=N_e}(Q, t=0). \quad (A4)$$

Note that a^4/τ has the same units as Wl^4, and in the formulation for $S(Q,t)$ used in Ref. 11, it is implied that the values of these two are equal. While this seems to work reasonably well to explain the full shape of $S(Q,t)$ for entangled polyethylene, it obviously does not do so for other entangled polymers, as is illustrated below.

APPENDIX B: PARAMETRIZATION FOR PURE LONG-PE AND OTHER ENTANGLED POLYMERS

In order to be usable in practice, the scattering functions of both the short (or any other type of polymer architecture molecules) and the long polymer must be entered in terms of a suitable model function into the RPA procedure. For that purpose, it is only necessary that the model interpolates the scattering function faithfully over an extended time range and the covered Q-range, preferentially with a small number of adjustable parameters. A physical model is of course preferable, but often not available. In the first step of determining the pure scattering function, the focus must be set to an
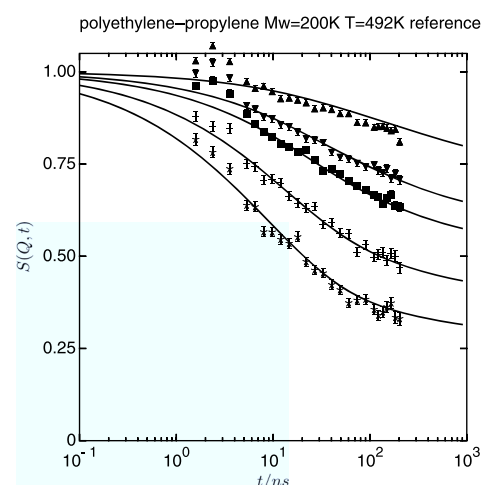

FIG. 6. Representation of the pure long-PI (polyisoprene) scattering function using Eqs. (A3) and (A4) by fitting IN15 NSE data from 80 kg/mol polyisoprene at T = 413 K.[21] Q-values are 0.051 Å^{-1}, 0.078 Å^{-1}, 0.096 Å^{-1}, 0.121 Å^{-1}, and 0.148 Å^{-1}. Global parameters are a = 159.0 Å, τ = 535 126.4 ns, R_e = 46.77 Å, and $W_x l^4$ = 4094.1 Å^4/ns, and the result is insensitive to L, which was fixed to 10.

accurate interpolation. Ideally, this is achieved by a physical model, and the parameters of it can then be determined directly. Otherwise, the RPA procedure is used to extract a proper interpolation representation of the pure scattering function (of the labeled compound), and this can be considered as the "evaluated" experimental result and as such be used to test it against model predictions. As Figs. 3 and 4 illustrate, a direct comparison of models of pure scattering functions with the experimental data at finite concentrations would

FIG. 5. Representation of the pure long-PE scattering function using Eqs. (A3) and (A4) by fitting older data[11,12] from 36 kg to 190 kg/mol PE, with T = 509 K. Q-values are 0.03 Å^{-1}, 0.05 Å^{-1}, 0.077 Å^{-1}, 0.096 Å^{-1}, and 0.115 Å^{-1}. Global parameters are a = 54.546 Å, τ = 206.86 ns, R_e = 34.93 Å, and Wl^4 = 36 812 Å^4/ns, and the result is insensitive to L, which was fixed to 90. These serve to communicate the pure long chain scattering function $S_{long}(Q,t)$ to the RPA procedure. For that purpose, they may be considered as mere inter/extrapolation means. The lines shown here are computed via the RPA procedure by setting the contrast to the long chains and reducing the concentration of other (short) chains to virtually zero. This implies the intermediate step of representing the result of (A3) and (A4) by a sum of 4–6 simple exp-functions [see, e.g., Eq. (C1)].
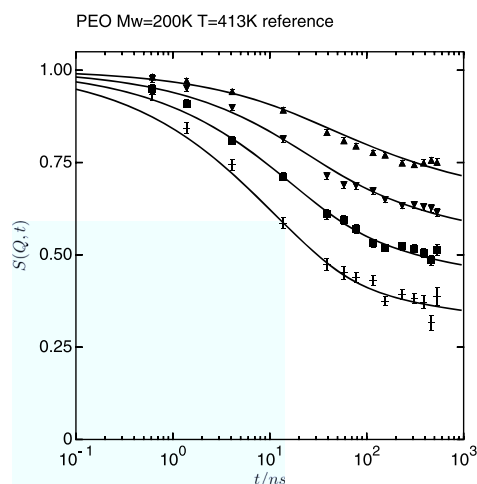

FIG. 7. Representation of the pure long-PEP (polyethylene–propylene) scattering function using Eqs. (A3) and (A4) by fitting IN15 NSE data from 200 kg/mol polyisoprene at T = 492 K.[22] Q-values are 0.05 Å^{-1}, 0.068 Å^{-1}, 0.077 Å^{-1}, 0.096 Å^{-1}, and 0.115 Å^{-1}. Global parameters are a = 70.6 Å, τ = 1321.5 ns, R_e = 40.02 Å, and $W_x l^4$ = 5157 Å^4/ns, and the result is insensitive to L, which was fixed to 10.
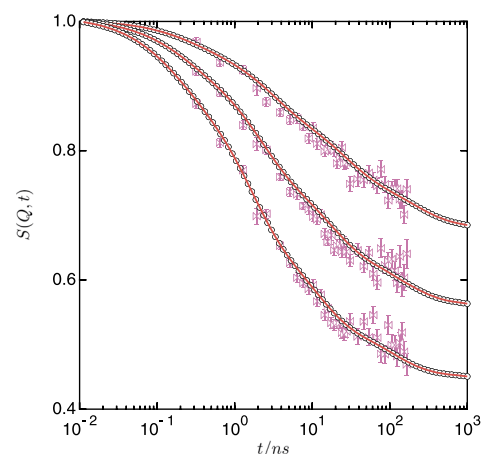
FIG. 8. Representation of the pure long-PEO (polyethyleneoxide) scattering function using Eqs. (A3) and (A4) by fitting IN15 NSE data from 190 kg/mol PEO at T = 413 K.[20,23] Q-values are 0.078 Å^{-1}, 0.096 Å^{-1}, 0.115 Å^{-1}, and 0.137 Å^{-1}. Global parameters are a = 53.1 Å, τ = 988.1 ns, R_e = 34.3 Å, and $W_x l^4$ = 2338 Å^4/ns, and the result is insensitive to L, which was fixed to 25.

FIG. 9. example for the accuracy of the automatic n-exponential representations. Shown here are the computation results of the reptation model function as in Fig. 5 for Q = 0.077, 0.096, and 0.115 Å^{-1} marked by open circles. The red lines show the representation by 5 (or 6 for the largest Q) simple exponentials. The magenta diabolos with error bars indicate the original data that served to fix the interpolation model parameters.

lead to erroneous results. The necessary input for the scattering function of the long chain "matrix" component for the interpretation of the experimental results of this paper was inferred from the data and fits shown in Fig. 5. As a convenient tool for investigation of mixtures containing entangled long chains of a number of NSE investigated polymers, we also show Figs. 6–8. The parameters shown in Table I can immediately be used to correspondingly modify the "matrix" functions in the examples contained in the software repository.

APPENDIX C: MAPPING OF MODEL FUNCTIONS TO THE SUM OF N EXPONENTIALS

The undisturbed (model) scattering functions $S^0_{nm}(Q, t)$ are required in a form, where the time dependence is described by a sum of exponentials, as follows:

$$S^0_{nm}(Q, t) = S_{nm}(Q) \times \left[\sum_{i=1}^{N} A_i(Q) \exp(-r_i(Q)t) \right]. \quad (C1)$$

To include this approximation step into fitting loops, it must be able to be unsupervised and must automatically yield accurate representations of the pure scattering functions that emerge from specific physical models. This is performed by a non-linear fit [Levenberg–Marquard (LM) in MINPACK] of the sum in Eq. (C1) to a table with n_p logarithmically spaced times $t_j = \exp[j \log(t_{max}/\Delta t)/n_p]\Delta t$, with Δt = initial step and maximum value: $t_{n_p} = t_{max}$. t_{max} should be chosen 2–3 times the maximum time covered in the experiment or desired theory description. Finally, the table contains values $f_j = S^0_{nm}(Q, t_j)/S^0_{nm}(Q)$ for parameters $\{(A_1, r_1)\cdots(A_N, r_N)\}$. The determination starts with $n > N$ tentative τ-values that are distributed with logarithmic spacing over the time range of the table. Using the table, the best amplitudes for this selection of characteristic times (rates) are then determined from the pseudoinverse from singular value decomposition. The resulting amplitudes and rates are then used as start values for a full nonlinear LM fit. The fit result is checked for "similar" rate values, and in case of a small (about 5%–20%) difference, adjacent values are combined to one $\sqrt{1/(\tau_i \tau_{i+1})} \rightarrow 1/\tau$; $(a_i + a_{i+1}) \rightarrow a$, and the effective number of exp-functions is reduced by one. Furthermore, components with

TABLE I. Parameters for the interpolation model for a number of long entangled polymers. These may be used to represent the $S(Q, t)$ of the pure polymer systems in the RPA procedure at least in the time range 0.1–1000 ns and 0.03 < Q < 0.15 Å^{-1}.

Polymer	M_w (kg/mol)	T (K)	a (Å)	τ (ns)	a^4/τ (Å^4/ns)	L	R_e (Å)	$W_x l^4$ (Å^4/ns)
PE	36 and 190	509	54.546	206.86	42 793	90	34.9	36 812
PI	80	413	159.0	535 126	1 194	10	46.8	4 094
PEP	200	413	70.6	1 321.5	18 806	10	40.0	5 157
PEO	190	413	53.1	988.1	8 046	25	34.3	2 338

rates faster than a predefined limit r_∞ (i.e., $r_\infty = 1/t_1$) are discarded. The new set again enters the LM-fit procedure as new start values. This is iterated until the number of remaining significant exp-functions stays constant. This procedure can be inside an (outer) fitting loop to determine model parameters of the "undisturbed" scattering functions. The validity of the model mapping fit result [Eq. (C1)] is checked after each step, and excess deviations are detected to create a warning. An example/check of the approach is illustrated in Fig. 9. Here, the model functions for the reptating chains [Eq. (A4) and Fig. 5] are computed into tables with 100 log-spaced time values between 0.01 ns and 1000 ns (open circles) that served as input for the procedure used to determine the approximation with simple exponentials [Eq. (C1)]. As a result, the procedure yields 5 or 6 exponentials. The resulting representation for $S(Q, t)$ is shown by the thick red lines in Fig. 9. Over the full time range, the deviations between the original model and the n-exp model are negligible.

REFERENCES

[1] D. Richter, M. Monkenbusch, A. Arbe, and J. Colmenero, "Neutron spin echo in polymer systems," Neutron Spin Echo Polym. Syst. **174**, 1–221 (2005).

[2] J. Colmenero and A. Arbe, "Recent progress on polymer dynamics by neutron scattering: From simple polymers to complex materials," J. Poly. Sci. Part B **51**, 87–113 (2013).

[3] D. Richter, "Neutron spin-echo investigations on the dynamics of polymers," Mol. Cryst. Liq. Cryst. **180**, 93–100 (1990).

[4] B. Ewen, "Neutron spin echo investigations of polymer dynamics," Curr. Opin. Solid State Mater. Sci. **3**, 606–609 (1998).

[5] G. Jannink and P. de Gennes, "Quasielastic scattering by semidilute polymer solutions," J. Chem. Phys. **48**, 2260–2265 (1967).

[6] A. Akcasu, M. Benmouna, and H. Benoit, "Application of random phase approximation to the dynamics of polymer blends and copolymers," Polymer **27**, 1935–1942 (1986).

[7] A. Akcasu and M. Tombakoglu, "Dynamics of copolymer and homopolymer mixtures in bulk and in solution via the random phase approximation," Macromolecules **23**, 607–612 (1990).

[8] L. N. G. Filon, "On quadrature formula for trigonometric integrals," Proc. R. Soc. Edinburgh **40**, 38–47 (1928).

[9] See https://doi.ill.fr/10.5291/Ill-Data.9-11-1895 for Institut Laue Langevin, Grenoble.

[10] D. Richter, R. Butera, L. Fetters, J. Huang, B. Farago, and B. Ewen, "Entanglement constraints in polymer melts: A neutron spin-echo study," Macromolecules **25**, 6156–6164 (1992).

[11] P. Schleger, B. Farago, C. Lartigue, A. Kollmar, and D. Richter, "Clear evidence of reptation in polyethylene from neutron spin-echo spectroscopy," Phys. Rev. Lett. **81**, 124–127 (1998).

[12] A. Wischnewski, D. Richter, M. Monkenbusch, L. Willner, B. Farago, G. Ehlers, and P. Schleger, "Reptation in polyethylene-melts with different molecular weights," Physica B **276**, 337–338 (2000) [2nd European Conference on Neutron Scattering (Ecns 99), Budapest, Hungary, September 01–04, 1999].

[13] P. G. de Gennes, "Coherent scattering by one reptating chain," J. Phys. **42**, 735–740 (1981).

[14] M. Doi and S. Edwards, *The Theory of Polymer Dynamics*, International Series of Monographs on Physics Vol. 73 (Oxford University Press, Oxford, 1994).

[15] R. A. L. Vallee, W. Paul, and K. Binder, "Probe molecules in polymer melts near the glass transition: A molecular dynamics study of chain length effects," J. Chem. Phys. **132**, 034901 (2010).

[16] T. Ge, G. S. Grest, and M. Rubinstein, "Nanorheology of entangled polymer melts," Phys. Rev. Lett. **120**, 057801 (2018).

[17] W. Paul, "Anomalous diffusion in polymer melts," Chem. Phys. **284**, 59–66 (2002).

[18] G. Smith, W. Paul, M. Monkenbusch, and D. Richter, "A comparison of neutron scattering studies and computer simulations of polymer melts," Chem. Phys. **261**, 61–74 (2000).

[19] C. Bennemann, J. Baschnagel, W. Paul, and K. Binder, "Molecular-dynamics simulation of a glassy polymer melt: Rouse model and cage effect," Comput. Theor. Poly. Sci. **9**, 217–226 (1999).

[20] B. J. Gold, W. Pyckhout-Hintzen, A. Wischnewski, A. Radulescu, M. Monkenbusch, J. Allgaier, I. Hoffmann, D. Parisi, D. Vlassopoulos, and D. Richter, "Direct assessment of tube dilation in entangled polymers," Phys. Rev. Lett. **122**, 088001 (2019).

[21] B. Gold, "Chain and association dynamics of supramolecular polymers," Ph.D. thesis, Westfälische Wilhelms Universität Münster, Münster, Germany, 2016.

[22] M. Monkenbusch, A. Wischnewski, L. Willner, and D. Richter, "Direct observation of the transition from free to constrained single segment motion in entangled polymer melts," Physica B **350**, 214–216 (2004) [3rd European Conference on Neutron Scattering (ECNS 2003), Montpellier, France, September 03–06, 2003].

[23] See https://doi.ill.fr/10.5291/ILL-Data.9-11-1773 for Institut Laue Langevin, Grenoble.